

DEVELOPMENT OF CYBER DUMMY FOR EVALUATING HUMAN BODY DAMAGES IN SEISMIC HAZARDS

F. Nagashima,¹ J. Ozaki,² E. Ikuta³ and M. Miyano⁴

¹ Professor, Graduate School of Urban Environmental Sciences, Tokyo Metropolitan University, Japan
Email: fumio-n@ecomp.metro-u.ac.jp

² Kanagawa Construction Center, Tokyo Electric Power Company, Inc., Japan

³ Assistant Professor, Graduate School of Human Life Science, Osaka City University, Japan

⁴ Professor, Graduate School of Human Life Science, Osaka City University, Japan

ABSTRACT :

One of the most important problems in investigations of natural disasters such as earthquakes and man-made disasters such as collisions between automobiles or ships or accidents involving crowds is to elucidate the mechanisms underlying injury or death. The ultimate purpose of this research is to present the development of a finite element anthropometric model (cyber dummy) that provides more accurate data about trauma than the current crash dummies used in automotive safety engineering. Ethical issues and the complicated shapes of the parts of the human body are considerable obstacles to the creation of cyber dummies. In this research we propose a procedure for transforming data and producing finite elements to create just such a model. Commercially available anthropometric data (DXF format) is processed, enabling closed spline curves to be used to fit the morphology of any given body structure. These closed spline curves are then automatically meshed in a standard application for producing a finite element model. The resulting solid model can be used to analyze trauma incurred during events such as collisions.

KEYWORDS: Cyber Dummy, Biomechanics, Anatomy Geometric Data, FE-Model Generation Method, Kinesiology, Disaster Mitigation

1. INTRODUCTION

Anthropometric dummies (physical representations of the human body) are expected to be useful for explaining the mechanisms of trauma to the human body in natural disasters such as earthquakes. In reference [1], the validation of a dummy (Hybrid-II) is described, which was originally created for use in the simulations of automobile front-end collisions and collapse of a two-story wooden house. The Hybrid-II showed some drawbacks, however. As with typical dummies for automobile accident simulations, their body parts were so hard and tough that reliable measurements could not be carried out. This could not be solved by redesigning the dummy with a flexibility more closely resembling that of the human body, and because the model could not withstand repeated reuse, the testing costs could become prohibitive. These practical considerations complicate the conduct of such simulations to explain mechanisms of injury.

Numerical models of the body can be used as replacements for physical dummies. Numerical simulations are already in use in the field of impact biomechanics to validate the safety of automobile passengers in accidents. Finite element models (FEMs) have previously been constructed using masses representing each human body part, as in conventional multi-body systems, but nearly all current simulations in advanced research use models containing deformable elements that are rather more faithful to the physical characteristics of the human body. We have published the results of investigations employing “virtual dummies” consisting of shell-and-beam elements to model the thorax²⁻⁴⁾. This requires the inclusion of softer tissues such as muscles and organs to obtain more accurate models, so a partially automated process for filling complicated shapes with solid elements must be developed.

The objective of this research is to develop a cyber dummy⁵⁾ that is less expensive and more accurate than

currently available models. This cyber dummy must be usable in a variety of situations involving trauma besides natural disasters, such as accidents involving public transportation or crowds. The present cyber dummy is an initial prototype, and is designed to provide the precision allowed by the capacity of a typical PC and was investigated in terms of the methods for withdrawing physical data, semi-automated meshing methods including those for soft tissue, transformation of data into a form readable by commercially available analysis software, and other factors.

2. CURRENT CAPABILITIES OF CYBER DUMMIES IN NUMERICAL SIMULATIONS

Among the models of the entire body are the H model and the THUMS from the Toyoda Central R&D Labs, which are run on the standard impact simulation package PAM-CRASH. These models have several drawbacks, however, because parts of the meshes are quite coarse, strict limitations for using these models are imposed, and they are expensive. Almost no one has used the currently existing cyber dummies for modeling the human body during disaster events.

Despite advances in the capabilities of hardware, such as the recent growth in multi-core processor technology, capabilities remain inadequate to provide satisfying accuracy in large anthropometric models. This study employed a computer with a dual-core CPU (3.6 GHz) and 3.0 GB of memory, and used the multipurpose FEM code LS-DYNA. This analysis system is restricted for use within approximately 200,000 finite elements. The main current use of such anthropometric models is to predict injuries due to physical loads typical of collisions. These predictions are accurate for injuries to comparatively tough structures such as bone, but are less dependable for parts consisting of soft tissue, such as organs. If only an organ is modeled, rather than the complete body, stress concentrations and other characteristics of the organ can be predicted, but researchers will have to wait longer for the development of computers that allow the prediction of phenomena occurring during collisions (injuries, tearing of internal organs, etc.). Since large amounts of labor and time are necessary to create models of the human body, beginning the preparations for those efforts now is appropriate.

3. METHODS FOR MODELING WITH CYBER DUMMIES

3.1. Morphological Data

Detailed morphological data are required to create an accurate FEM of the human body, but taking three-dimensional measurements of the shapes of structures such as muscles and bones is very laborious. Modeling the body by computed tomography, magnetic resonance imaging (MRI), and other such methods would expose subjects to health risks owing to various forms of electromagnetic radiation. Nearly all of the necessary morphological information is quite difficult to obtain. Some limited data are available, both commercially and at no cost. One of the free numerical human morphology databases is provided by the Applied Electromagnetic Research Center, an independent administrative agency in Japan. This database was created to calculate the effects of electromagnetic waves on the body when someone is using a cell phone and was compiled using cross-sectional images from MRI for mean body sizes of adult Japanese males and females. The elements comprise cubes of 2 mm size on each side. The total number of elements in the male model is 44,339,200 ($320 \times 160 \times 866$). These elements are then classified into over 50 types, such as bone, heart and lungs. At present, however, the analysis using this immense number of elements is impossible using a PC, and the data must be pre-processed to reduce the number before any actual analyses can be carried out. If a user can obtain a commercially available anthropometric database, this will usually be in the form of a three-dimensional computer graphics file. These data include whole-body files, as well as models of limbs or other parts. Other products are also available, from aircraft to animals and furniture. For this report, a whole-body model that included internal organs and other features was obtained. That model was then modified to develop a FEM of the human body. All the body parts were simulated with triangular 3D-Surface elements, for a total of 271,512 elements and 227,980 vertices. The elements were classified into 230 types to represent different types of muscle, organs, bones, etc. According to the data for body length and weight of Japanese of different age cohorts published in the 2003 National Health and Nutrition Survey in Japan, the average height of 20-year-old Japanese individuals is 1,710 mm. For this study, a body of 1,716 mm height was generated, on the basis of our original data. The morphological database did not provide any information on weight, so the body weight was set at 64.2 kg f, the average for 20-year-old Japanese individuals as of 2003.

3.2. Transformation of Anthropometric Data

The obtained morphological data were in the .DXF format, and thus it had to be transformed in order to be used as finite elements. A program was written in Java to transform these elements into a format that could be read by the standard analytical code LS-DYNA. This program included 5 classes (Viewer, CosmosReader, DxfReader, DynaReader and DynaWriter) and was capable of booting the computer program, supplying a GUI environment, and reading and writing in all of the files. DXF files must contain at least Header, Table, Block and Entity sections. The drawing data are stored in the Entities section; the triangular 3DFACE can also be placed in Entities. The DXF format places point data on two lines per point. The first line is an integer called the “Group Code”, and the value determines the format of data on the second line. For example, “100” indicates that the second line is a character string, while numbers in the 10-59 range indicate floating point numerical values. Table 1 shows the Group Codes used for 3DFACE elements. Here, “AcDbFace” means that the element is three-dimensional. The data indicate locations of the four vertices of the element - when the element is a thick triangle, the 3rd and 4th points have the same coordinates.

Table 1: Group codes in 3DFACE elements

Group code	Comments
100	Subclass marker (AcDbFace)
10, 20, 30	Coordinates of 1st vertex on face (x, y, z)
11, 21, 31	Coordinates of 2nd vertex on face (x, y, z)
12, 22, 32	Coordinates of 3rd vertex on face (x, y, z)
13, 23, 33	Coordinates of 4th vertex on face (x, y, z)

3.3. Method for creating solid muscle elements

Figure 1 shows an example of the partially automated procedure for creating solid elements in which part of the thigh (here, the femoral muscle) was modeled. The data after transformation to DYNA format ① was for triangular shell elements, like the original data. It is necessary to create solid elements to fill the spaces among the 3D-surfaces of the femur and femoral muscle, which have surfaces that are defined with triangular shell elements. Meshing these body parts is nearly impossible, no matter what techniques are employed, because the meshes are of very different sizes and the meshing conditions are very different. We conceived a method of cutting the femur and femoral muscle surfaces into cylindrical slices at appropriate spacings and approximating the cross-sectional shapes with closed spline curves ②. Once this group of closed splines ③ had been created, they were connected with a closed surface called a “loft” ④ in SolidWorks. Once at this stage, basic element length can be selected as appropriate and the loft can be meshed automatically with tetrahedral elements ⑤.

- ① Original data converted to LS-DYNA format
- ② Approximation with spline curves
- ③ Conversion to SolidWorks data format
- ④ Verification of loft shape
- ⑤ Re-meshing with solid elements

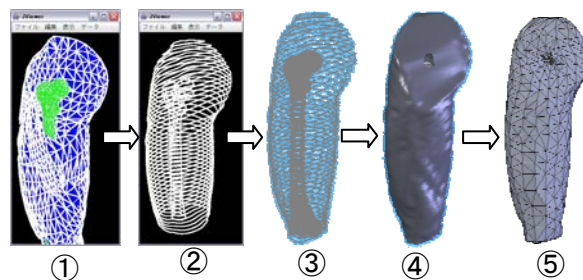


Figure 1 Flow of semi-automated meshing of soft tissue

3.4. How to define closed spline curves

These closed spline curves are created using a series of points on the outline of a cross-section. The point series data comprise the spatial coordinates for both ends (p and q) of the line defined by the intersection of the triangular shell element ABC with cutting plane Π (Fig. 2). The data were obtained using the following procedure:

- 1) Dot products of the vector normal to the cross-sectional face with the vectors from each of the sides of the triangular element determine whether the lines can intersect.
- 2) When intersection is possible, it is determined whether each respective intersection lies on the side itself; if so, then the coordinates of the intersection are saved.
- 3) The above mentioned tasks are performed for all the elements making up the body part. The vertex data set describing the cross-sectional shape (the polygon) on the cutting plane surface is generated.

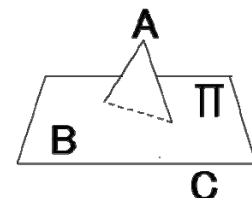


Figure 2 Diagram of creation of a data set for the spline curve

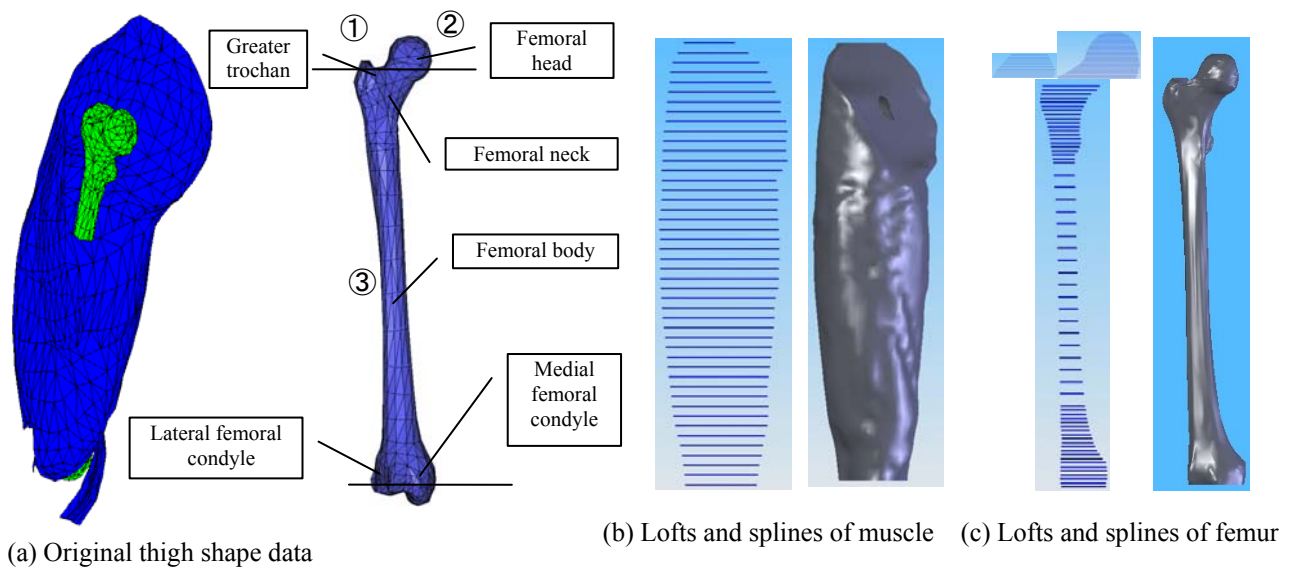


Figure 3 Process of creating lofts of the femur

As special cases, when the triangular element and cut cross-section are given in parallel, or when these lie on the same plane, they are handled as not having any intersecting points. The obtained series of points is transformed into SolidWorks format and outputted. A program was written in Java to perform the above series of tasks. The five classes and two packages (Cross, Element) described in 3.(2) above were defined. These two classes comprised eight and five classes, respectively. In Figure 1, step ② (partway through the calculation process) shows how the spline curve can be used to describe the cross-section.

3.5. Semi-automated production of mesh (Example I, modeling the thigh)

The original data (Fig. 3(a)) for the thigh were processed by slicing as shown in (b) and (c) to obtain the spline shape data. These were then used to create the loft version of the thigh. The upper part of the thigh is forked. The larger branch with the ball-shaped portion is the femoral head, and the smaller branch is the greater trochanter. Multiple splines may not be created on the same cross-sectional face, so there is an issue of how to perform the loft of this section. A cross-section was taken just below the fork and new series of cross-sections and lofts were created to simulate the two branches. The lower end of the femur is also divided at the knee joint into medial and lateral condyles. Here, however, the muscular cover is thin, and there seems to be little need to create a solid model of it, so this muscular tissue was neglected in the model.

As Figure 3 shows, the femur was divided into 3 sections: ① greater trochanter, ② femoral head, and ③ femoral body. Splines were made for each of these parts. Appropriate to the local morphology, the numbers of slices were 9, 31, and 59 (19 + 20 + 20), respectively.

The loft function allows the volumes to be attached to or detached from each other. The loft created for this femur model is shown in Figures 3(b) and 3(c), but removing the femoral muscle model leaves a hole where the bone was. Lofts are thus created in the method described above. Next, a reference element length d_e is defined and the volumes are meshed with tetrahedral elements. Figure 4 shows how a thigh was meshed in 7 stages with $d_e = 17-28$ mm. The numbers of nodes and elements in successive models are given in the figure. The model could not be meshed with d_e of any lengths greater than 28 mm. Elements tended to be small when lofts with complicated shapes are meshed. For $d_e = 17-20$ mm, the number of elements was reduced by approximately 1200 for each increase of d_e by 1 mm. This reduction then became about 560 elements per 1 mm increase for $d_e = 20-26$ mm. Almost no reduction in the number of elements or nodes was observed at $d_e = 27$ or 28 mm. The minimum total number of elements created in the loft shown in Figure 3 appeared to converge at about 6,080. The mesh is easy to apply once the loft is made, so future advances in computers will be sufficient to enable the determination of the desired d_e . In this study, the model with $d_e = 27$ mm was employed.

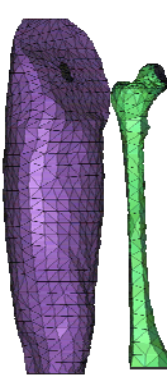
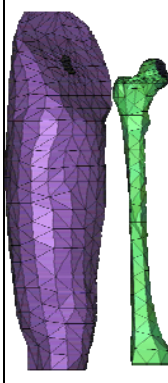
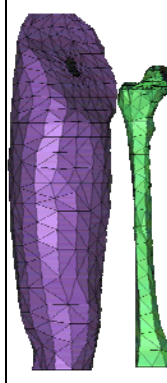
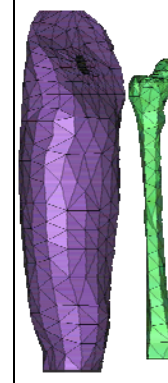
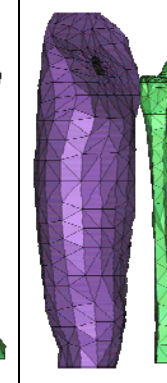
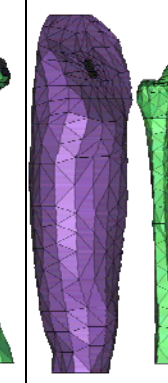
d_c : 17mm	20mm	24mm	25mm	26mm	27mm	28mm
						
2896 nodes 13360 elements	1955 nodes 9736 elements	1511 nodes 7534 elements	1398 nodes 6946 elements	1293 nodes 6374 elements	1237 nodes 6107 elements	1229 nodes 6082 elements

Figure 4 Example of automated-meshing for femoral muscle and femur (d_c : reference element length)

3.6. Semi-automated production of mesh (Example II, modeling the hip)

The main bones making up the hip are the pelvic bone and the sacrum. Together, the hip bones and sacrum make up what is called the pelvis. To model the pelvic region, a loft is created in the shape of the soft tissue, beginning from the surface of the hip bone. The region taken up by the bones is then removed. Compared with long bones like the femur and tibia, the hip bone and sacrum display much more complex shapes, requiring a more complicated procedure for creating lofts.

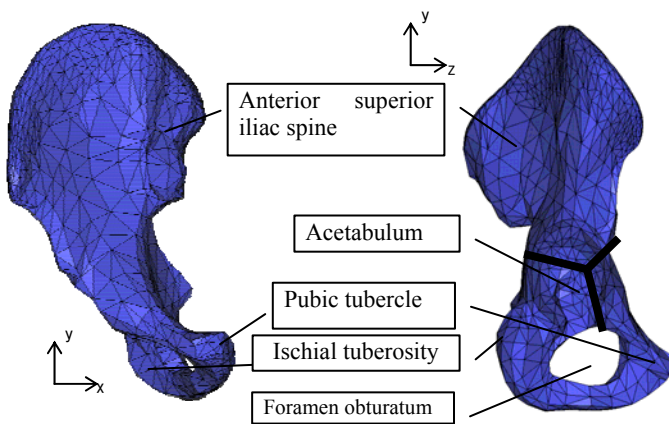


Figure 5 Shape of pelvic bone

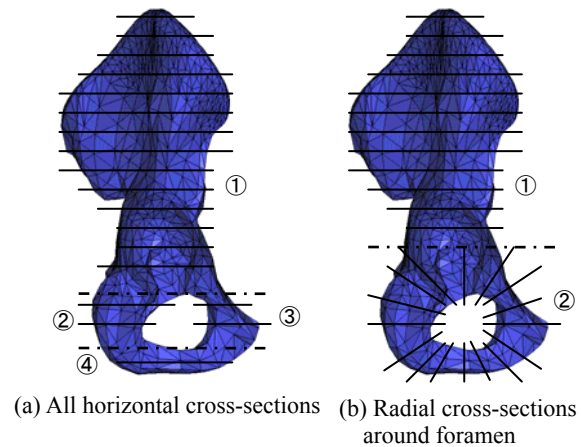
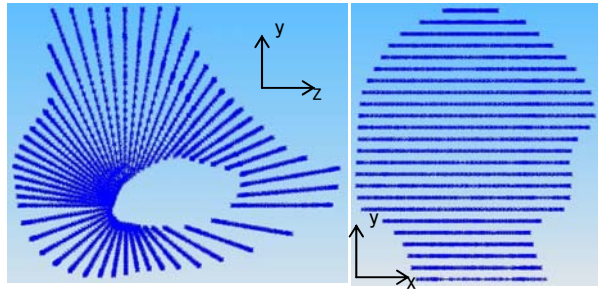


Figure 6 Layout for locations of spline curves

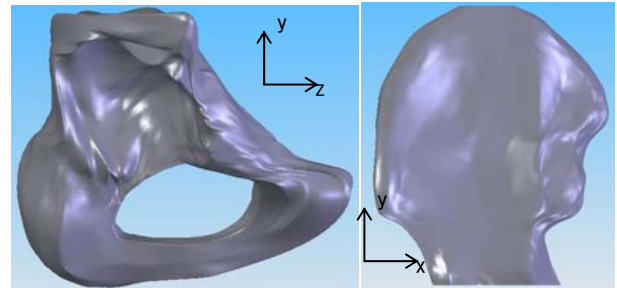
Figure 5 shows morphological data for the right hip bone. The hip bone consists of the ilium, pubis, and ischium and begins to form by the 3rd fetal month from a cartilage called the “Y-shaped cartilage” because of its shape. The Y-shaped cartilage is replaced by bone in the 18th to 20th year of life, and the ilium, pubis and ischium fuse to form what is called the “pelvic bone”. The former components are then called the “anterior superior iliac spine”, “ischial tuberosity” and “pubic tubercle”. A spherical depression is visible when the pelvic bone is viewed from the side. This depression is called the “acetabulum”, and makes up the hip joint when the femoral head is seated within. A ring is formed in the lower part of the pelvic bone by the ischial tuberosity and pubic tubercle; this ring is called the “foramen obturatum”. In the initial attempt to create lofts of the pelvic bone, the bone was divided into the four portions as shown in Figure 6(a) and these were each sliced parallel to the z-x plane. However, this approach resulted in complicated shapes near the foramen and the lofts did not model the bone shape accurately. The pelvic bone was then modeled in the two upper and lower portions shown in Figure 6(b). The lower part surrounding the foramen obturatum, consisting mainly of the ischial tuberosity and pubic tubercle, was sliced on radial planes approximately normal to the tangential lines of the foramen. Figure 7(a)

shows spline curves generated during slicing. The initial point and vector for the axis of rotation for the section plane were entered. Planes were created at 10° increments in the lower portion surrounding the foramen, where the shape was fairly simple, and at 5° increments in the upper portion, where the shape was complicated. The upper portion of the hip bone was cut in 23 planes parallel to the z-x plane at 5-mm intervals.



(a) Splines in lower half of hip bone (b) Splines in upper half of hip bone

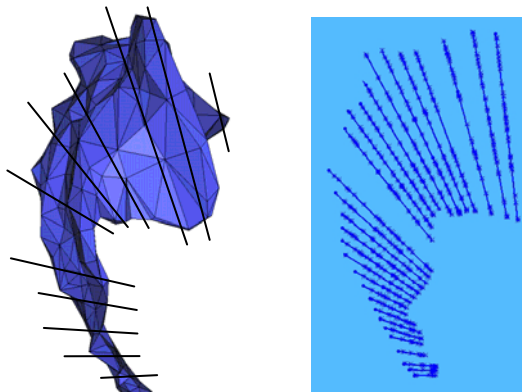
Figure 7 Splines used for hip bone



(a) Loft of lower half of hip bone (b) Loft of upper half of hip bone

Figure 8 Lofts of hip bone

Figure 8 shows the lofts obtained for the lower and upper halves of the pelvic bone. Some mismatch was observed at the connection between the two lofts. This discrepancy could have given rise to errors later, when combined volumes were meshed, and thus, they had to be leveled. The cross-section at the bottom of the upper half was adjusted to match the top of the lower half. The sacrum, like the pelvic bone, is formed by the fusion of several smaller bones. Toddlers display five vertebrae beneath the lumbar vertebrae, but later in life, these combine to create the sacrum. The sacrum contains 4 pairs of holes called the anterior and posterior sacral foramina. Ordinarily, the shape of these foramina would be of concern, but these foramina are so small that they were neglected in the sacrum model.



(a) Sections of sacrum (b) Spline of sacrum

Figure 9 Spline of sacrum

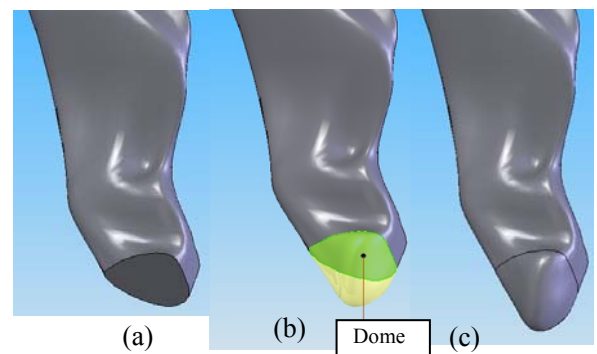


Figure 10 Tip of the tailbone in simulation

Figure 9 shows a side view of the sacrum, which is approximately arc-shaped. Accordingly, section planes of the sacrum were placed along vectors normal to tangent lines along the arc. A model of the sacrum was made by creating lofts from these splines, but as shown in Figure 10(a), the tip of the tailbone was not accurately represented. A drawing feature called a “dome” was employed to obtain the pointed tip. A dome adds a protruding volume to a defined flat location (Figs. 10(b) and 10(c)).

4. CREATING AN ANTHROPOMETRIC REPRESENTATION OF THE RIGHT SIDE OF THE BODY

Space does not permit us to show the processes for creating FE versions of other body parts here, but it is possible to create meshed models of the feet, shins, upper arms, hands, thorax, head and other parts using the same procedures as shown above for the thigh and pelvic region. An attempt was made to create an anthropometric model of just the right side of the body, for the simplicity of calculation. The human body is not exactly left-right symmetrical, but half can be modeled and then mirrored to obtain an approximate model of the entire body.

4.1. Lower limb model

A model of the lower limb was made by combining thigh, shin, pelvis, and foot with hip, knee and ankle joints. The spherical joint and revolute joint elements shown in Figure 11 were used to connect the body part models.

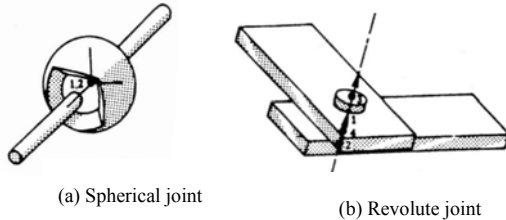


Figure 11 Elements used in joints of model

The joints were defined with the limits (Fig. 12) in the extension and inflection directions, defined as positive and negative, respectively, and with viscous resistance and non-linear rotational resistance curves.

4.2. Upper limb model

The upper limb model consisted of the upper arm, forearm and hand. An elbow joint was inserted between the upper arm and forearm, and a wrist joint was inserted between the forearm and hand. The wrist is a condyloid joint and allows inflection, extension, eversion (radial flexion) and inversion (ulnar deviation). No twisting motion is imparted at the actual wrist joint itself, the palm of the hand is turned by a rotation of the radius, i.e., motion at the radioulnar joint. According to reference [6], the movable angles of the wrist joint are 70-90° in inflection, 65-85° in extension, 12-25° in abduction, and 25-40° in adduction. The wrist joint was therefore simulated with a spherical joint between the models of the hand and the radius (Fig. 13). The spherical motions must be constrained, so the rigid-body model derived from the Generator of Body Data (GEBOD) was used.

4.3. Thorax and head model

The thorax and head model consists of 24 vertebrae and 12 other bones, comprising the ribs, rib cartilage, sternum, clavicle, shoulder blade, skull and mandible. The rib cartilage, sternum and ribs were joined at nodes. The tough ligaments between the ribs and vertebrae were modeled with shell elements. The thoracic cage and clavicle are connected by the sternoclavicular and costoclavicular ligaments. The sternoclavicular ligaments tie the upper portion of the sternum, and the costoclavicular ligaments tie the first rib cartilage, to the proximal tip of the clavicle. These ligaments were also modeled with shell elements (Fig. 14), as were the

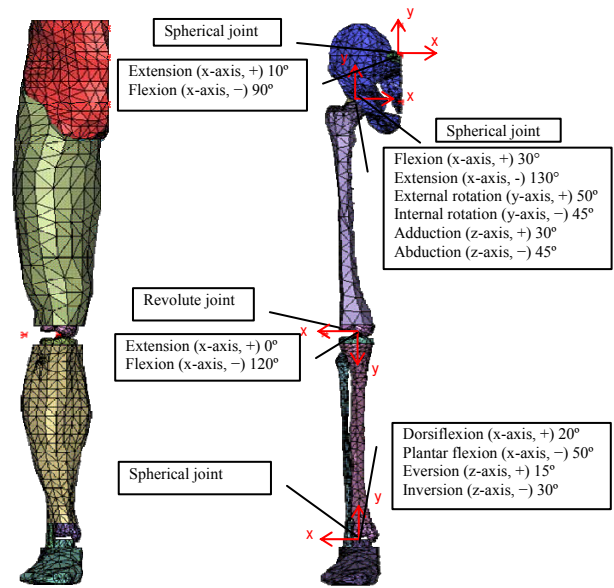


Figure 12 Model of right leg connected at joints

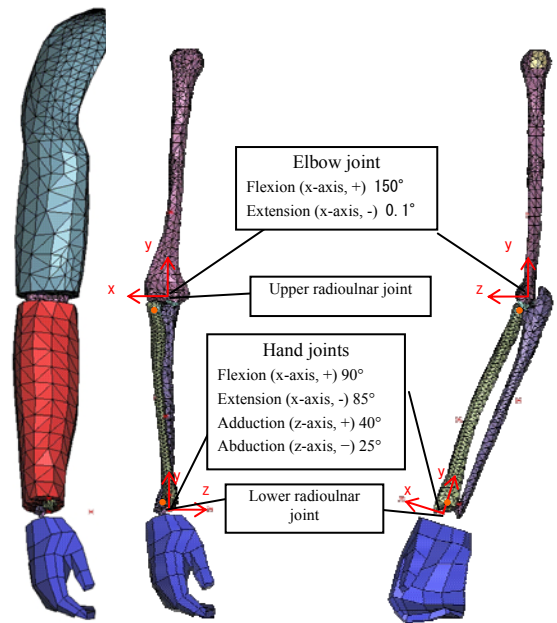


Figure 13 Upper limb models

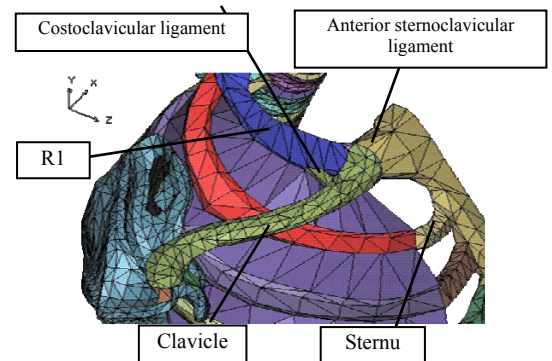


Figure 14 Thorax model

ligaments connecting the clavicle with the shoulder blade: the acromioclavicular, conoid and trapezoid ligaments.

Figure 15 shows front and rear views of the head and thorax models. Ball joints were inserted to connect the thoracic vertebrae. Resistance to motion in intervertebral articulation was represented by a torque that varied linearly with a fixed stiffness, once it had reached the value corresponding to the frictional resistance moment.

Pin joint elements with a stop angle of 37° were used at the mandibular joint in the skull. Muscle tissues such as external abdominal oblique, sternocleidomastoid and scalene muscles were also added as shell elements.

5. SUMMARY

Some essential technologies for creating FE anthropometric models were developed. One of the essential technologies was how to obtain morphological data about the human body and transform this into usable formats. Input data were in DXF format and had to be transformed into the format of LS-DYNA, which was the commercially available analysis software used here. The application for performing that transformation was written in Java. A semi-automated meshing procedure was developed for meshing volumes with soft tissue. Solid-modeling of muscle tissue is a considerable challenge for creating anthropometric models for FEM. In this paper, we present a solution to that problem. Models were successfully filled with three-dimensional solid elements using an automated meshing application. Anthropometric data had to be re-constructed using the lofting function to employ the automated meshing function, and an application was developed to perform this. A set of other procedures was also established to transform the data to that for standard analysis software, such as for obtaining a mesh of muscular tissue with solid elements.

Future studies will address how to improve the accuracy of this model by gathering data on the physical properties of organs and investigating mechanical characteristics and behaviors during failure.

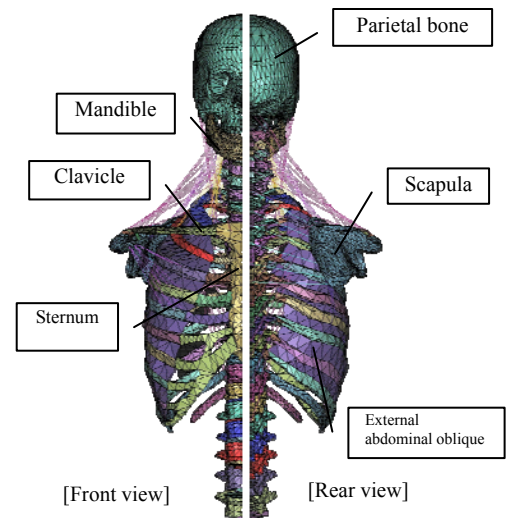


Figure 15 Thorax and head model

ACCKNOWREGEEMENT

This research was partially supported by the Ministry of Education, Science, Sports and Culture, Grant-in-Aid for Scientific Research (C), 18560468, 2006-2008.

REFERENCES

- 1) M. Miyano, et al. "A basic study on simulation of human casualties by the finite element method." Proceedings of the Fourth Civil Engineering Symposium on Progress in Earthquake and Natural disaster based on processes to prevent collapse of structures, March, 2003 (In Japanese).
- 2) M. Miyano, E. Ikuta, F. Nagashima et al.: "A basic study on simulation of human casualties by the finite element method (Part 2)" Proceedings of the Fourth Civil Engineering Symposium on Progress in Earthquake and Natural disaster based on processes to prevent collapse of structures, March 2003 (In Japanese)
- 3) E. Ikuta, M. Miyano, F. Nagashima et. al.: Measurement of the Human Body Damage Caused by Collapsed Building, 13th World Conference on Earthquake Engineering, DVD-ROM Paper ID628, Vancouver, B.C., Canada, 2004.
- 4) E. Ikuta, M. Miyano, Fumio Nagashima and Jun Ozaki: Framework of Biomechanical Modeling for Evaluating Human Body Damages Caused by Collapsed Building in Great Earthquake, First European Conference on Earthquake Engineering and Seismology, ID-1815 (CD-ROM), Geneva, Switzerland, Sep. 2006ID-1815.
- 5) J. Ozaki and F. Nagashima: Framework of Generating Cyber Dummy FE-Model for Evaluating Human Body Damages, JSCE Journal of Earthquake Engineering, Vol.29, Earthquake Engineering Committee, JSCE, Aug., 2007 (In Japanese).
- 6) C. W. Thompson and R. T. Floyd: Manual of Structural Kinesiology (Fifteenth Edition), McGraw-Hill, 2004..